Journal of Inflammation Research

Dovepress
open access to scientific and medical research

Open Access Full Text Article

ORIGINAL RESEARCH

MULT1-Encoding DNA Alleviates Schistosomiasis-Associated Hepatic Fibrosis via Modulating Cellular Immune Response

Lu Yang[1,*], Li Sun[1], Yalan Cao[1], Qi Wang[1,2], Anni Song[1], Ru Zhu[1], Wenqi Liu[1], Shengjun Lu[1,*]

[1]Department of Pathogen Biology, School of Basic Medicine, Tongji Medical College, Huazhong University of Science and Technology, Wuhan, People's Republic of China; [2]Department of Histology and Embryology, School of Basic Medicine, Guizhou Medical University, Guiyang, People's Republic of China

*These authors contributed equally to this work

Correspondence: Shengjun Lu; Wenqi Liu, Department of Pathogen Biology, School of Basic Medicine, Tongji Medical College, Huazhong University of Science and Technology, Wuhan, 430030, People's Republic of China, Tel +86 15307159688; +86 13886014791, Fax +86-27-83692608, Email Lushengjun@hust.edu.cn; liu_wq2002cn@hotmail.com

Purpose: In schistosomiasis-associated hepatic fibrosis, the role of murine UL16-binding protein-like transcript 1 (MULT1), the strongest ligand of natural killer group 2-member D receptor (NKG2D), remains unclear. Here, *Schistosoma japonicum*-infected mice administered with MULT1-encoding DNA were used to test MULT1 as a potential therapy for schistosomiasis-associated hepatic fibrosis and explore relevant mechanisms.

Materials and Methods: A recombinant plasmid encoding MULT1 (p-rMULT1) was constructed and administered to *Schistosoma japonicum*-infected BALB/c mice via hydrodynamic tail vein injection. Egg granulomas in liver, hepatic fibrosis biomarkers and levels of cytokines were investigated. Comparisons of CD4+ T, CD8+ T, NK and NKT proportions as well as their phenotype were performed not only between *Schistosoma* infected, p-rMULT1 treated group and *Schistosoma* infected, backbone plasmid pEGFP-N1 treated group but also between infected, nontreated group and health control group.

Results: Reduced area of granuloma formation and fibrosis around single eggs, downregulated expression of collagen I, α-smooth muscle actin, TGF-β and IL-10, and upregulated expression of IFN-γ, were observed in the livers of p-rMULT1 treated mice. p-rMULT1 treatment improved *Schistosoma* infection impacted immune microenvironment by modulating proportion of $CD4^+$ T $CD8^+$ T, natural killer (NK) and NKT cells, enhancing expression of NKG2D, in lymphocytes, and augmenting IFN-γ secretion by $CD4^+$ T, $CD8^+$ T, NK and NKT cells, as well as partially reversing some other phenotype changes of lymphocytes.

Conclusion: To the best of our knowledge, we provided the first in vivo evidence that MULT1 is a favorable anti-fibrosis factor in the context of schistosomiasis. The inhibitory effect of MULT1 overexpression on schistosomiasis associated with hepatic fibrosis may result from augmenting the proportion and function of NKG2D-expressing immune cells, and from enhancing NK- and T-cell activation, as well as regulating the helper T (Th)1/Th2 balance.

Keywords: schistosomiasis, NKG2D, liver fibrosis, IFN-γ, natural killer cells, T lymphocytes

Introduction

Schistosomiasis is a helminthic infectious disease, affecting ~258 million individuals in 78 countries.[1,2] *Schistosoma mansoni* and *Schistosoma japonicum* infection can cause severe liver fibrosis induced by eggs trapped in the liver. At 4–6 weeks after being infected by *S. japonicum*, patients enter the chronic infection stage, in which the eggs are excreted and partially deposited into the liver. The deposited eggs release soluble egg antigens, which trigger extensive infiltration by monocytes, eosinophils, neutrophils and lymphocytes, leading to granulomatous immune-pathogenesis lesion.[3,4] Activated hepatic stellate cells (HSCs) during the persistent lesion transformed into fibroblasts to help heal and produce

Received: 17 January 2022
Accepted: 7 July 2022
Published: 16 July 2022

large amount of extracellular matrix, including collagen fibers, more than that can be degenerated by tissue proteinase, resulting in fibrosis at the granuloma site.[3,4]

Helper T (Th) 2 immune response driven by IL-4, IL-5, IL-10 and IL-13 is the most prominent immune response observed during liver fibrosis.[5–7] IL-4 and IL-5 antibody treatment can significantly suppress liver fibrosis in mice.[8] In IL-4 gene-deficient mice, absolute IL-4 absence makes acute lethal inflammation occur after schistosomiasis, accompanied by severe hepatic and intestinal damage.[9,10] IL-13 stimulates the activation and differentiation of HSCs into fibroblasts and facilitates fibrosis.[11,12] Evidence both from patient and from mouse model indicates that IL-13 is a strong accelerator for the progress of liver fibrosis after *Schistosoma* infection.[13,14] IL-4, IL-10 and IL-13 can also stimulate macrophage transformation into alternatively activated macrophages, which are a major source found in inflammatory zone protein 1/resistin-like molecule-α, favoring the conversion of HSCs into fibroblasts.[15] At 12 weeks after infection, the Th2 immune response is downregulated, which may be attributed to IL-10 and TGF-β inducing regulatory T cells to regulate the balance of the Th1/Th2 response.[5,6,16] In addition, the newly formed granuloma area around the eggs is reduced, suggesting that liver fibrosis can be ameliorated by suppressing Th2 response. IFN-γ can inhibit Th2 cell proliferation[17] and selectively promote Th1 cell differentiation.[18] Furthermore, previous studies have shown that IFN-γ can suppress fibrosis by inhibiting the HSC activation and TGF-β signaling.[19,20]

Natural killer group 2 member D receptor (NKG2D), a C-type lectin-like membrane receptor, is an activating receptor expressed on the surface of a wide range of effector cells, such as natural killer (NK), NKT, $CD8^+$ T and γδ T cells.[21,22] Once bound to its ligands on the cell surface, NKG2D conducts signals via the DNAX-activating protein 10 and/or DNAX-activating protein 12 to the effector cells and promotes their proliferation, cytokine secretion and cytotoxicity.[23] NKG2D signaling plays critical roles in antitumor and anti-infection immunity, as well as in some autoimmune diseases, such as contact hypersensitivity.[24–27] A limited number of studies indicated its involvement in *S. japonicum* infection and consequent hepatic fibrosis. Hou et al[28] observed an increased transcript of several retinoic acid early transcript (RAE)-1 members, but not of minor histocompatibility antigens encoded by locus *H60* or murine UL16-binding protein (ULBP)-like transcript 1 (MULT1) in HSCs during weeks 6–8 post-infection with *S. japonicum*. Gong et al[29] reported a correlation between the presence of *MICA*A5*, a truncated form of the MHC class I chain-related family molecules (*MICA*) allele, which encodes a human NKG2DL protein, and the degree of schistosomiasis-associated fibrosis. Due to their critical role in immune stimulation, NKG2D and its ligands are considered as promising potential targets for regulating immunity against tumors, infections and autoimmune diseases.[30,31] Considering that the MULT1 ligand binds to its receptor with greater affinity than other ligands for NKG2D,[32] it may hold promise as a tool for limiting liver fibrosis induced by *Schistosoma* eggs. Therefore, in order to test NKG2D ligands as a potential therapy for schistosomiasis-associated hepatic fibrosis, a plasmid encoding recombinant MULT1 (p-rMULT1) was constructed and administered to *S. japonicum*-infected BALB/c mice. It was investigated whether overexpression of MULT1 in vivo could suppress the progression of liver fibrosis induced by schistosomiasis. The effects of treatment on the proportion and function of NKG2D-expressing immune cells, such as NK, NKT and $CD8^+$ T cells, and the Th1/Th2 shift were also investigated, in the hope of elucidating the mechanism underlying the anti-fibrosis effect of MULT1 in schistosomiasis mice.

Materials and Methods

Ethics Approval

All experimental procedures involving mice were in compliance with the Chinese Council on Animal Care and approved by the Institutional Animal Care and Use Committee, Huazhong University of Science and Technology (IACUC no. 2568).

DNA Construction

To generate p-rMULT1, full-length cDNA encoding MULT1 (GenBank No. BC132070.1, 1155 base pairs) was amplified from a cDNA library of mouse liver infected with *S. japonicum* by using PCR. Error-free amplified cDNA was identified by sequencing, tailed with a haemagglutinin (HA) tag-encoding sequence at the 3'-end (5'-TAC CCA TAC GAT GTT CCA GAT TAC GCT-3'), and then subcloned into the eukaryotic expression vector pEGFP-N1 (Addgene, Inc.).

In vitro Expression of rMULT1

293T cells (ATCC, CRL-3216) were cultured in DMEM (HyClone; Cytiva) supplemented with 10% FBS (HyClone; Cytiva) and 1% penicillin–streptomycin solution (MilliporeSigma). p-rMULT1 (1 μg) in 50 μL serum-free DMEM medium and 10 μL Lipofectamine® 2000 (Thermo Fisher Scientific, Inc.) in 50 μL serum-free DMEM were mixed gently, incubated at room temperature for 20 minutes and then applied to 293T cells (70% confluence in 24-well plate). After a 2-h incubation at 37 °C, 5% CO2, the supernatant was replaced with 0.5–1 mL DMEM containing 10% FBS and 1% penicillin–streptomycin solution. Another pEGFP-N1-based construct encoding a truncated form of MULT1 was used as a control plasmid, whose product lacks the band of 50 kDa, the molecular mass weight of rMULT1, on the Western blot assay membrane. After 48 h, transfected 293T cells were lysed in RIPA lysis buffer (cat. no. 89901; Thermo Fisher Scientific, Inc.) for further analysis.

Mouse and Parasites

Mice and *S. japonicum*-infected *Oncomelania hupensis* snails were purchased from the Hubei Provincial Center for Disease Control and Prevention (Wuhan, China). Mice were maintained at room temperature of 22–26°C, 40–50% relative humidity with 12-h light/dark cycle and free access food and water, under specific pathogen-free conditions. Animal infection and sacrifice were performed under anesthesia by intraperitoneal administration of tribromoethanol (250 mg/kg).

Challenging with S. Japonicum

For infection, six-week-old BALB/c mice were percutaneously infected with 24*S. japonicum* cercariae per mouse by putting cercariae harbored wet cover slips on the shaved abdominal skin while under anesthesia. Infected mice without any treatment were used as infected group and mice with mock procedures, which were handled almost the same way except that no cercariae on the wet cover slips were used as healthy control.

Treatment with p-rMULT1, Serum and Tissue Harvesting

For the treatment experiment, 12 infected mice were randomly divided into two groups at the end of 4th week post infection, p-rMULT1 (40 μg/mouse) was intravenously administered weekly for 4 weeks by hydrodynamic tail vein injection.[33,34] Vehicle vector pEGFP-N1, instead of p-rMULT1, was used as the control (GFP-ctl). Mice were weighted twice weekly. Prior to sacrificing the mice, serum was collected via the tail vein as well as cardiac puncture under anesthesia. The livers, kidneys, colons and spleens were harvested and processed for further analysis. Livers and spleens were weighed prior to being processed.

H&E and Masson's Trichrome Staining

Neutral formalin-fixed, paraffin-embedded Swiss rolls of colon and tissues from kidney, spleen, as well as the left hepatic lobe were cut into 4-μm sections and stained with hematoxylin and eosin (H&E) or Masson's trichrome stain. To perform granuloma size measurements, five single egg-induced granulomas were randomly selected from each sample (magnification x200). The sizes of granulomas were measured using the MSHOT Image Analysis System. In addition, tissues stained with Masson's trichrome stain were used to assess the collagen deposits of fibrosis. At least five images (magnification x200) were captured from each sample, and the images were quantified using the MSHOT Image Analysis System. The fibrotic area was determined by using the ratio of collagen deposition area to total area.

Flow Cytometry Analysis

Spleens were meshed through a 100-μm cell strainer in ice-cold RPMI-1640 medium (HyClone; Cytiva) supplemented with 2% FBS. Single splenocytes suspensions were purified by removing red blood cells using Red Cell Lysis Buffer (cat no. RT122-02; Tiangen Biotech Co., Ltd.).

The liver tissue for infiltrating lymphocytes isolation was meshed through a 100-μm cell strainer in ice-cold RPMI-1640 medium and then separated from hepatocytes by centrifugal mixing with 35% isotonic Percoll. The single-cell suspension was treated with Red Cell Lysis Buffer to remove red blood cells.

For surface staining, a total of 2×10^6 cells were stained in 0.01 M PBS containing 2% FBS for 30 min at 4 °C, with the following fluorescence labeled anti-mouse specific antibodies: CD3 (clone 145–2C11; eBioscience; Thermo Fisher Scientific, Inc.), CD4 (clone RM4-5; BD Biosciences), NKp46 (clone 29A1.4 eBioscience; Thermo Fisher Scientific, Inc.) and NKG2D (clone CX5; eBioscience; Thermo Fisher Scientific, Inc.), CD49b (clone DX5; BD Biosciences), CD27 (clone LG.7F9; eBioscience; Thermo Fisher Scientific, Inc.;), CD62L (clone MEL-14; eBioscience; Thermo Fisher Scientific, Inc.;) and killer cell lectin-like receptor G1 (KLRG1; clone 2F1/KLRG1; BioLegend, Inc.;).

For intracellular cytokine staining, lymphocytes were stimulated with 50 ng/mL polymethacrylate (BD Biosciences), ionomycin (1 μg/mL, BD Biosciences) and GolgiPlug reagent (20 μL/mL, BD Biosciences) at 37°C for 6 h prior to staining with surface antibodies. These cells were then fixed and permeabilized with Fixation/Permeabilization Kit according to the manufacturer's protocol (BD Biosciences), and incubated with fluorescence labeled anti-IFN-γ (clone XMG1.2; eBioscience; Thermo Fisher Scientific, Inc.) and anti-IL-4 (clone 11B11; eBioscience; Thermo Fisher Scientific, Inc.;). The ratio of IFN-γ^+ to IL-4^+ was used as Th1/Th2 ratio.

Dead cells were excluded by applying the fixable viability dye eFluor 506 (eBioscience; Thermo Fisher Scientific, Inc.). All antibodies were used at an optimal concentration after titration. Gating of cells was based on the specific isotype control as well as fluorescence minus one (FMO) setting when needed. The analyses of stained cells were performed by using FACSVerse or LSRII (BD Biosciences). Data were analyzed by using FlowJo 10 software (FlowJo LLC). Geometric mean fluorescence intensity (MFI) over the entire peak was used to measure the expression of interested molecules.

Cytometric Bead Array (CBA)

Concentration of IFN-γ, IL-17, TNF-α, IL-2, IL-4 and IL-6 in plasma as well as in liver tissue were measured using CBA (BD Biosciences) according to the protocols provided by the manufacturer and analyzed by using a FACSVerse or LSRII flow cytometer. A standard curve was drawn from the MFI of the standard, and the concentration of each cytokine was calculated based on the standard curve. The concentration of liver local cytokines was expressed as mass per milligram tissue.

Aminotransferase Measuring

Serum alanine aminotransferase (ALT) activity was measured using commercial kits (Nanjing Jiancheng Bioengineering Institute, Nanjing, China) according to the manufacturer's guide.

Western Blot Assay

Liver tissue lysates or lysates of transfected 293T cells, with each loading sample containing 30 μg total protein (Determined by Bradford assay), were analyzed by using 12% SDS-PAGE gel. Resolved proteins were electro-transferred to polyvinylidene difluoride (PVDF) membranes. The membranes were blocked for 2 h with 5% nonfat milk at room temperature and then probed with antibody specific to HA Tag (ProteinTech Group, Inc.), collagen I (ABZoom Inc.), α-smooth muscle actin (α-SMA; ProteinTech Group, Inc.), TGF-β (ProteinTech Group, Inc.), GAPDH (ProteinTech Group, Inc.) or β-actin (ProteinTech Group, Inc.).

Sandwich Fluorescence Immunoassay

Sandwich fluorescence immunoassay[35] was modified and employed to evaluate the protein concentration of MULT1 in the liver. Briefly, nonionic latex beads (Invitrogen; Thermo Fisher Scientific, Inc.) were coated with 25 μg/mL MULT1 monoclonal antibody (clone 5D10; eBioscience; Thermo Fisher Scientific, Inc.) and blocked with 2% bovine serum album and then incubated with liver tissue lysates and then captured MULT1 was detected by staining with fluorescence labeled detecting antibody specific for MULT1 (clone 237104, R&D Systems, Inc.) and analyzing on FACSVerse or

LSRII flow cytometer. A standard curve was drawn from the MFI of the standard recombinant MULT1 protein (R&D Systems, Inc.) and the concentration of MULT1 was calculated based on the standard curve. The level of liver local MULT1 was expressed as the mass of MULT1 per gram liver tissue.

Reverse Transcription-Quantitative PCR (RT-qPCR)

Total RNA was extracted from liver tissues by using the TRIzol reagent (Biosharp Life Sciences) and reverse transcribed by using a ReverTra Ace qPCR RT Kit (Toyobo Life Science). Then, the cDNA was analyzed for the expression of transcription levels of various genes with SYBR Premix Ex Taq™ on a MyiQTM2 Real Time System (Bio-Rad Laboratories, Inc.). The thermocycling program comprised 94°C for 5 min, 40 cycles of 30 s at 95°C and 60°C for 30 s, and a final extension for 5 min at 72°C. Fold amplification was normalized by GAPDH and the primers used were as follows: GAPDH, 5'-primer: GTGTTTCCTCGTCCCGTAG and 3'-primer: ATGGCAACAATCTCCACTTT; IFN-γ, 5'-primer: AGTGGCATAGATGT GGAA and 3'-primer: CTGATGGCCTGATTGTC; TGF-β, 5'-primer: CCCACTGATACGCCTGAG and 3'-primer: GGGCTGATCCCGTTGAT; IL-10, 5'-primer: CAACATACTGCTAACCGACTCCT and 3'-primer: TGAGGG TCTTCAGCTTCTCAC; α-SMA, 5'-primer: GAGCGTGAGATTGTCCG and 3'-primer GCTGTTATAGGTGGTTTCG; collagen I, 5'-primer: GGCGGTTCAGGTCCAAT and 3'-primer: TCGGTGTCCCTTCATTCC; and Mult1, 5'-primer: GTCTGTGTCCAAGGATAGAAGAG and 3'-primer: AAAGAGGCTGTCTGTTGAGTAG

Statistical Analysis

Comparisons of means are performed between infected group (infected) and health control group (NC) or between p-rMULT1 treated group (rMULT1) and vehicle plasmid treated group (GFP-ctl). Statistical significance was assessed by independent samples unpaired Student's *t*-test using Prism GraphPad Prism 7 Software (GraphPad Software, Inc.). All experiments were conducted for 3 times independently. Data were expressed as the means ± SEMs. $P < 0.05$ was considered to indicate a statistically significant difference.

Results

Overexpression of rMULT1 Attenuates Murine Schistosomiasis Associated Hepatic Fibrosis

To investigate whether rMULT1 overexpression affects the progression of liver fibrosis, a pEGFP-N1-backboned plasmid encoding recombinant rMULT1, p-rMULT1, was constructed (Figure S1A, B and C) and was tested to be able to be expressed in eukaryotes (Figure S1D). At 4 weeks post infection with *S. japonicum*, each mouse in the experimental group was administered four doses of 40 μg p-rMULT1 in the following 4 weeks via hydrodynamic tail vein injection (Figure 1A). Compared with the vehicle plasmid (pEGFP-N1)-treated mice (GFP-ctl group), p-rMULT1 treated mice (rMULT1 group) showed significantly elevated mRNA (Figure 1B) and protein (Figure 1C) of MULT1 in their liver, demonstrating in vivo expression of the injected rMULT1 coding sequence. H&E and Masson's trichrome staining data revealed that the area of single egg granuloma was smaller (Figure 1D) and the collagen deposition was significantly reduced (Figure 1E) in the liver of the rMULT1 group compared with the GFP-ctl group. Similarly, the transcription levels of collagen I and α-SMA in the livers of mice treated with p-rMULT1 were also lower compared with those in the vehicle plasmid-treated group (Figure 1F and G). This indicated a reduction in the activation of HSCs and collagen fiber production, which was confirmed by Western blot assay (Figure 1H-J). The body weight change curve indicated that rMULT1 DNA treatment ameliorated body weight loss in the infected mice (Figure S2A), while both p-rMULT1-treated mice and pEGFP-N1-treated mice exhibited similar spleen and liver weights (Figure S2B and C). Neither significant survival difference nor serum ALT activity distinction was observed between the two groups (Figure S2D and E). Both groups have similar colon length (Figure S2F). No morphological difference was observed between p-rMULT1-treated mice and pEGFP-N1-treated mice, either in the colon, spleen or in the kidney (Figure S2G). These results suggested that overexpression of rMULT1 in the chronic phase of infection in mice can alleviate murine hepatic fibrosis induced by schistosomiasis and NKG2D-based immunity plays a protective role for schistosomiasis associated with liver fibrosis.

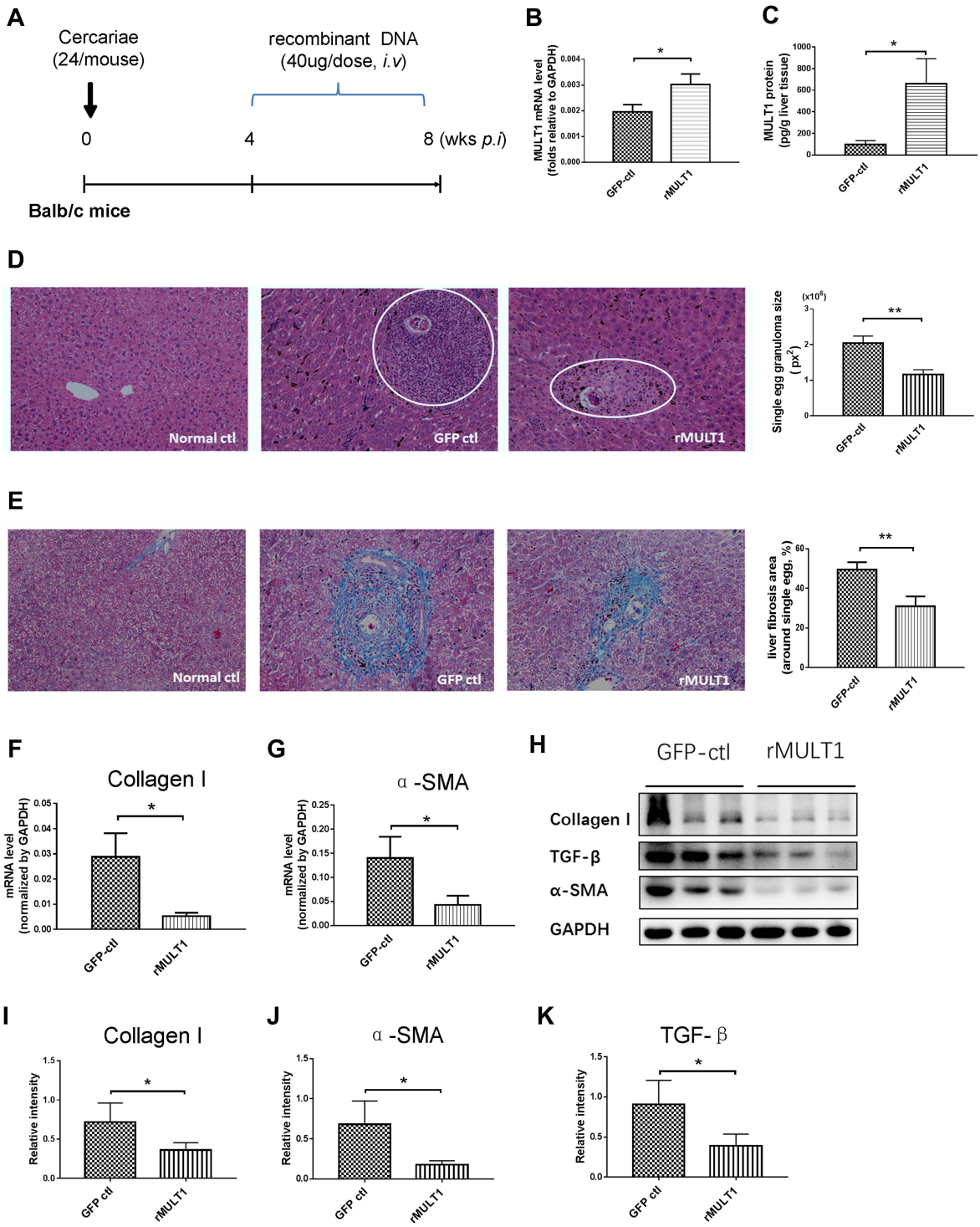

Figure 1 MULT1 encoding DNA injection alleviates egg granuloma and hepatic fibrosis in mice infected with *Schistosoma japonicum*. (**A**) Experimental design. Briefly, 6-week-old BALB/c female mice (n=6 per group) were artificially infected with *S. japonicum* by cutaneous contact with 24 cercariae on a wet cover slip. Administration of 40 μg rMULT1 DNA or vehicle DNA was carried out via hydrodynamic tail vein injection; the process was initialized at 4 weeks post infection and repeated 3 times in 1 month before the mice were anaesthetized and sacrificed at the end point. (**B**) RT-qPCR data and (**C**) sandwich fluorescence immunoassay showing elevated MULT1 expression in p-rMULT1-injected mice compared with control group mice (GFP-ctl) administered vehicle plasmids. (**D**) Representative H&E staining images (left panel, magnification x200) and quantification of mean (±SEM) egg-induced granuloma size in the liver (white circles). (**E**) Representative Masson's trichrome staining images (left panel, magnification x200) and quantification of mean (±SEM) collagen deposition (right panel). (**F** and **G**) RT-qPCR showing decrease of (**F**) liver collagen I and (**G**) α-SMA expression. Western blotting assay demonstrating reduced protein concentration of (**H** and **I**) collagen I, (**H** and **J**) α-SMA and (**H** and **K**) TGF-β in the livers of mice administered rMULT1 DNA. Data are representative of 4–6 animals per subgroup and 3 independent experiments. Comparisons were between rMULT1 and GFP-ctl, *P<0.05 and **P<0.01.
Abbreviations: MULT1, murine UL16-binding protein-like transcript 1; RT-qPCR, reverse transcription-quantitative PCR; SMA, smooth muscle actin; rMULT1, recombinant MULT1.

Treatment with p-rMULT1 Results in Elevated Liver IFN-γ Levels

The pathological damage and liver fibrosis in the chronic phase of schistosomiasis are caused by various immune and related cells, as well as various pro- and anti-inflammatory cytokines.[7,36,37] However, no difference was observed in the serum levels of IFN-γ, IL-2, IL-4, IL-6, IL-17 or TNF-α between the rMULT1 group and the GFP-ctl group (Figure 2A) using CBA assay. Both RT-qPCR and CBA assay detected an increase of IFN-γ expression in the livers of the rMULT1 group (Figure 2B and C). The mRNA levels of IL-10 in the p-rMULT1-treated group were lower compared with those in the GFP-ctl group (Figure 2B). There was no significant difference in the mRNA level of TGF-β between the two groups (Figure 2B), while a decreased liver TGF-β was detected in the treated group by Western blot (Figure 1H and K). Taken together, these data collectively suggested that rMULT1 overexpression promotes the expression of IFN-γ, but suppresses the expression of IL-10 and TGF-β in the liver.

NKG2D Expression is Enhanced and the Proportions of T Cells and NK Cells are Changed

NKG2D is the only receptor for rMULT1 and is expressed on the surface of $CD8^+$ T, NK and NKT cells. The expression of NKG2D on lymphocytes is associated with their status of activation and proliferation.[38,39] In mice with chronic infection with *S. japonicum*, the proportions of splenic $CD4^+$ T, $CD8^+$ T, NKT and NK cells sharply decreased (Figure 3A and B), so as that of hepatic ones (Figure 3C and D) except $CD8^+$ T cells. The percentage changes of these cells, except splenic $CD4^+$ T cells and liver NKT cells, were partially reversed by rMULT1 DNA treatment (Figure 4A-D). At the same time, chronic infection downregulated the expression of NKG2D in NK cells .(Figure 5A and G), splenic $CD8^+$ T cells (Figure 7A) and NKT cells (data not shown), and rMULT1 DNA treatment following infection elevated surface NKG2D of NK cells (Figure 6A and G), splenic $CD8^+$ T cells (Figure 8A) and NKT cells (data not shown). Meanwhile, NKG2D expression did not change in $CD4^+$ T cells (Figure 7F, 8F, 9G and H) and liver $CD8^+$ T cells (Figure 9A and B), either upon infection or in response to subsequent treatment. These results indicated that NKG2D expression of lymphocytes was impaired by long-term infection with *S. japonicum*, and overexpression of rMULT1 during infection can enhance NKG2D expression and restore the frequency of NKG2D expressing lymphocytes.

Overexpression of rMULT1 Enhances NK Cell Activation in Infected Mice

It was previously demonstrated that NK cells can modulate fibrosis during infection with *S. japonicum*;[28] however, NK function was impaired during the fibrotic stage of *Schistosoma* infection.[40] NKG2D binding to its ligands efficiently elicits the immune response of NK cells.[39] Flow cytometry analysis of splenic and hepatic NK cells was performed to observe their phenotype changes caused by infection and following treatment with p-rMULT1. In addition to NKG2D expression changes (Figures 5A and G), surface KLRG1 (Figure 5B and H), CD49b (Figure 5D and J) and intracellular IFN-γ expression (Figure 5E, F, K and L) decreased, while surface CD69 level increased (Figure 5C and I) in NK cells upon infection, and all these changes, along with NKG2D expression, were reversed by rMULT1 DNA administration (Figure 6A-L). These data indicated that, to an extent, rMULT1 DNA injection can restore NK cell activation and function in mice with chronic *S. japonicum* infection, favoring anti-fibrosis immunity.

p-rMULT1 Administration Affects T-Cell Phenotypes and Th1/Th2 Shift

It is well known that T lymphocytes serve a key role in the immune response against *Schistosoma* infection. On the other hand, T-cell immunity is markedly affected by schistosomiasis, particularly after the onset of egg deposition.[16,41,42] Using flow cytometry, several phenotypic changes in mouse T cells were observed, both upon infection and in response to p-rMULT1 administration, including IFN-γ levels and the expression of some surface molecules, such as NKG2D, KLRG1 (both in spleen and in liver), CD62L and CD27 in spleen (Figures 7–9). Along with the aforementioned changes in surface NKG2D (Figures 7A and 8A), KLRG1 and CD27 on splenic $CD8^+$ T cells ($CD3^+CD4^-$) as well as KLRG1 on liver $CD8^+$ T cells decreased in *Schistosoma* infected group compared to the health control group (Figure 7C, D and 9C), while p-rMULT1 treatment enhanced the expression of KLRG1 (Figures 8C and 9D) and CD27 (Figure 8D) on $CD8^+$ T cells. $CD4^+$ T cells have rarely been reported to express NKG2D, except in some specific disease context including rheumatoid arthritis (RA), Crohn's

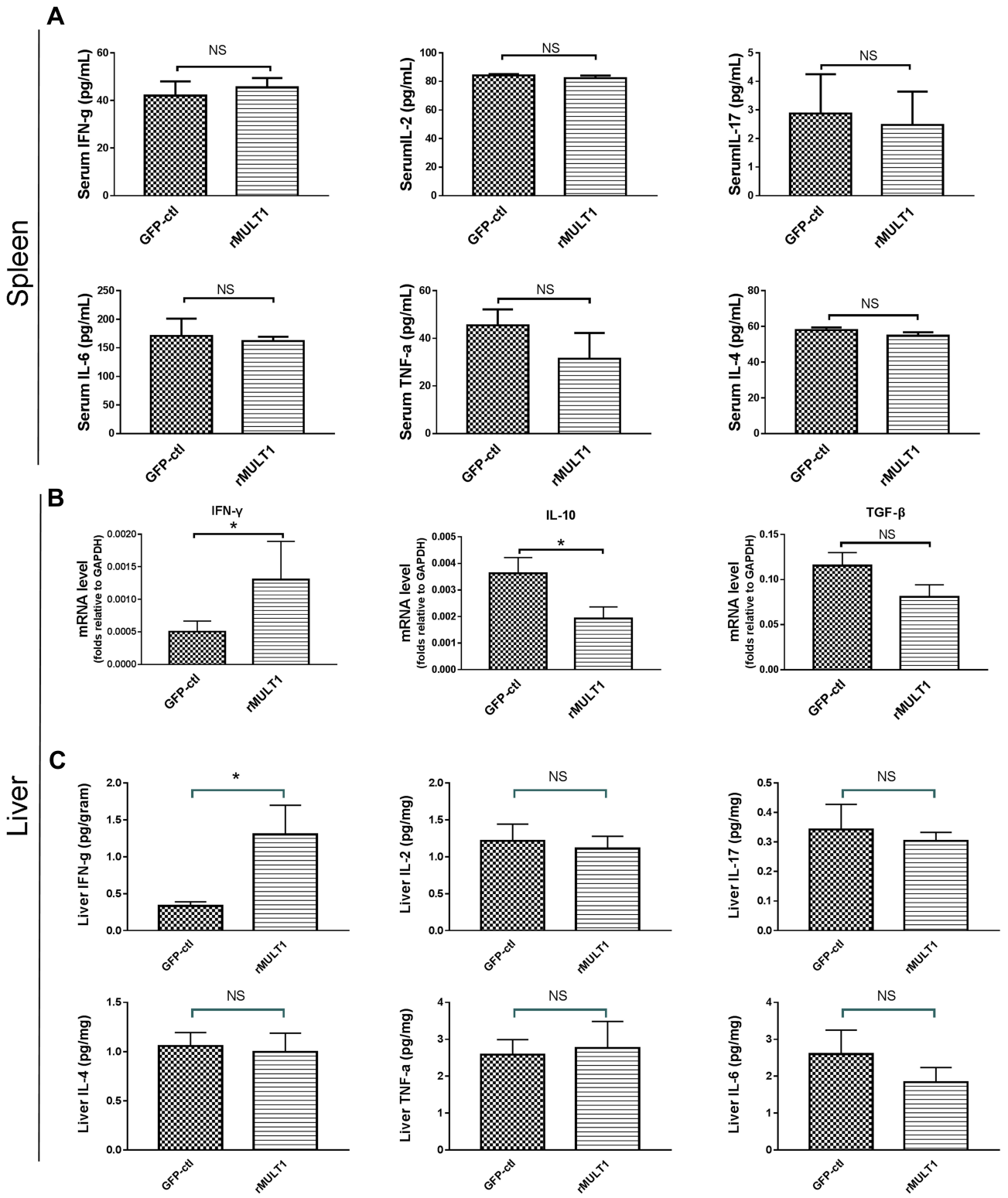

Figure 2 Cytokine levels in the serum and liver. (**A**) Cytometric bead array analysis showing similar levels of several serum cytokines between treated mice and GFP-ctl mice, including IFN-γ, IL-2, IL-17, IL-6, TNF-α and IL-4. (**B**) Reverse transcription-quantitative PCR showing increased IFN-γ, decreased IL-10 and similar TGF-β RNA levels in liver of the rMULT1 group relative to the GFP-ctl group. (**C**) Cytometric bead array analysis of liver tissue showing elevated IFN-γ, unchanged IL-2, IL-17, IL-6, TNF-α and IL-4 in treated group. Comparisons were between rMULT1 and GFP-ctl, *P<0.05.

Abbreviations: MULT1, murine UL16-binding protein-like transcript 1; rMULT1, recombinant MULT1.

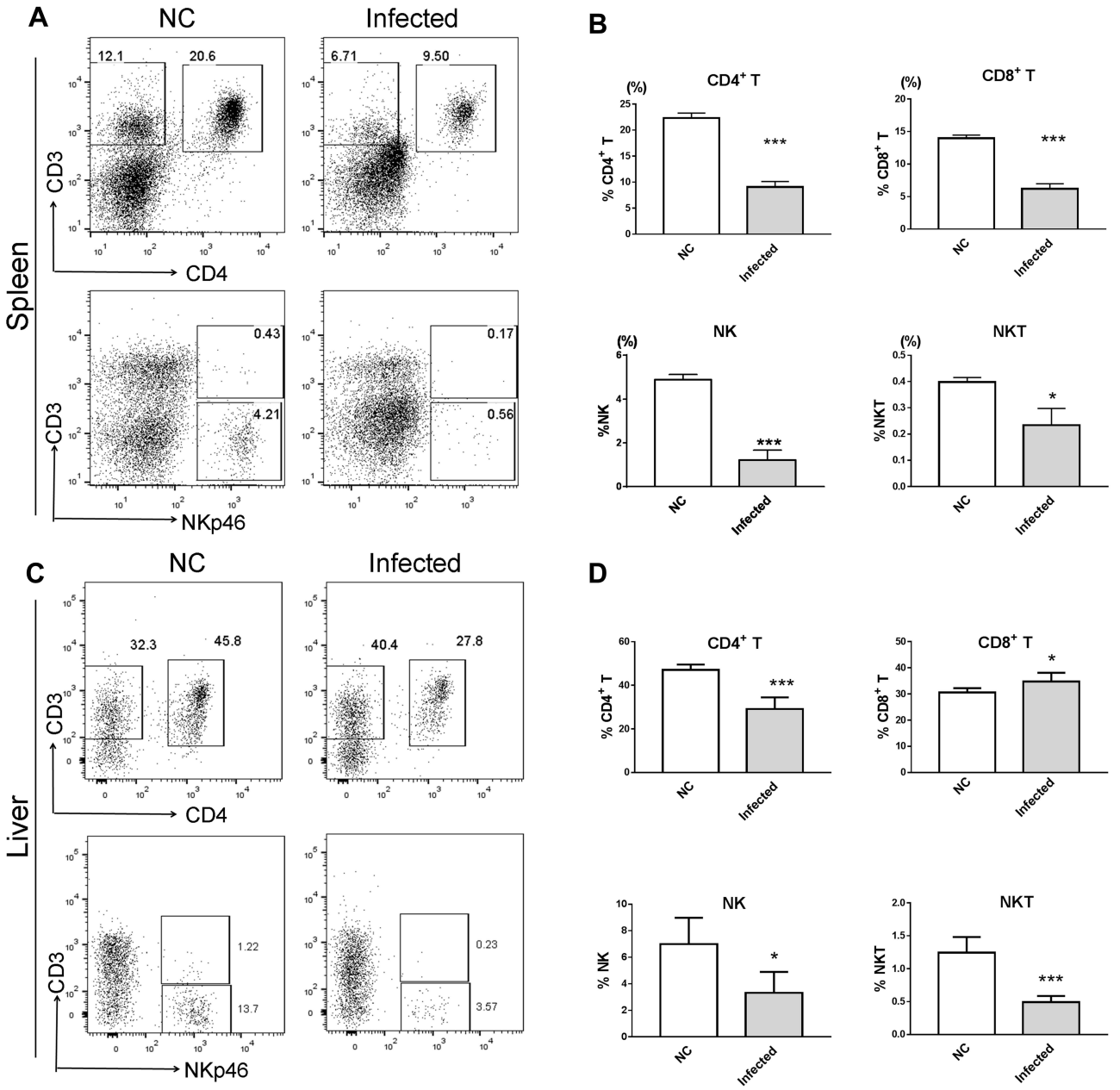

Figure 3 Decreased $CD4^+$ T, $CD8^+$ T, NK and $NKP46^+$ NKT cell percentages in the spleen and the liver of BALB/c mouse with chronic *S. japonicum* infection. BALB/c female mice aged 6 weeks were artificially infected with 24 cercariae of *S. japonicum* or served as the healthy control with a mock infection procedure, then without any treatment, mice were euthanized and data were collected at 8 weeks post infection. (**A** and **C**) Representative dot plot graphs and (**B** and **D**) summary data demonstrated a significantly decreased percentage of NK cells, $NKP46^+$ NKT cells, $CD8^+$ T cells and $CD4^+$ T cells in (**A** and **B**) splenocytes and (**C** and **D**) liver infiltrating lymphocytes of mice. Data are representative of 4–6 animals per subgroup and 3 independent experiments. Comparisons were between Infected and NC. *P<0.05 and ***P<0.001.
Abbreviations: MULT1, murine UL16-binding protein-like transcript 1; rMULT1, recombinant MULT1; NK, natural killer.

disease, type 2 diabetes, multiple sclerosis, and systemic lupus erythematosus (SLE).[43] Neither schistosomiasis nor p-rMULT1 treatment following *S, japonicum* infection changed surface NKG2D levels on murine $CD4^+$ T cells (Figures 7F, 8F, 9G and 9H). However, like $CD8^+$ T cells, $CD4^+$ T cells from p-rMULT1 treated mice also exhibited higher surface KLRG1 and CD27 expression compared with those from vehicle treated mice (Figures 8H, 8I and 9J), while the infection did not impact on expression of KLRG1 on splenic $CD4^+$ T cells (Figure 7H) but it suppressed CD27 expressing of splenic $CD4^+$ T cells (Figure 7I) and KLRG1 expression of hepatic $CD4^+$ T cells (Figure 9I). Although chronic *Schistosoma* infection impacted the expression of L-selectin, an important adhesion molecule that helps lymphocytes migrate to inflammatory sites, in both subsets of T cells (Figure 7B and G), after treatment with p-rMULT1, a further decrease in L-selectin was

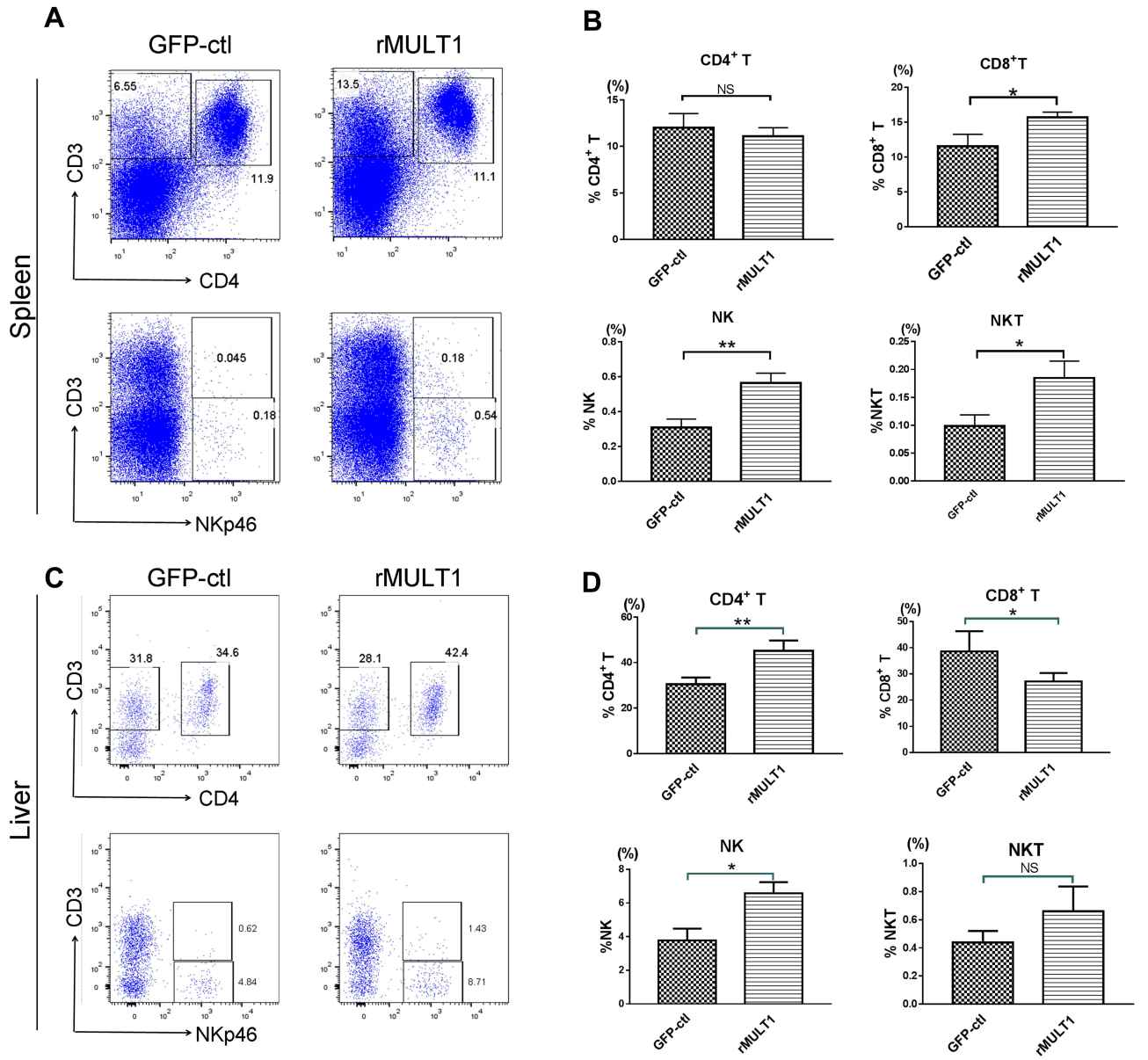

Figure 4 rMULT1 DNA restores lymphocyte percentages in the spleens and livers of *S. japonicum*-infected mice. (**A** and **C**) Representative dot plot graphs and (**B** and **D**) data demonstrated a significantly increased portion of NK cells, NKP46$^+$ NKT cells, CD8$^+$ T cells in spleen and of NK cells, CD4$^+$ T cells in liver but not of CD4$^+$ T cells in spleen or NKT cell in liver, as well as a significantly decreased portion of CD8$^+$ T in liver, of mice that received rMULT1 DNA treatment. Data are representative of 4–6 animals per subgroup and 3 independent experiments. Comparisons were between rMULT1 and GFP-ctl, *P<0.05 and **P<0.01.

Abbreviations: MULT1, murine UL16-binding protein-like transcript 1; rMULT1, recombinant MULT1; NK, natural killer.

only detected in CD4$^+$ T cells (Figure 8G), not in CD8$^+$ T cells (Figure 8B). Furthermore, long-term *Schistosoma* infection inhibited IFN-γ secretion of CD4$^+$ T cells (Figures 7J and 9K), of liver CD8$^+$ T cells (Figure 9E) but not of splenic CD8$^+$ T cells (Figure 7E), and rMULT1 DNA treatment enhanced IFN-γ secretion both in CD4$^+$ T cells (Figures 8J and 9L) and in CD8$^+$ T cells (Figures 8E and 9F).

During the progression of schistosomiasis, along with egg deposition and accumulation in the liver, Th2 response replaces Th1 response, becoming the dominant type of immune response, and facilitates liver fibrosis in the chronic phase of *S. japonicum* infection.[44,45] Our ex vivo co-staining of IFN-γ with IL-4 on CD4$^+$ T cells revealed restoration of the Th1/Th2 ratio in the rMULT1 DNA-treated group, both in spleen (Figures 7K and 8K) and in liver (Figure 9M and N).

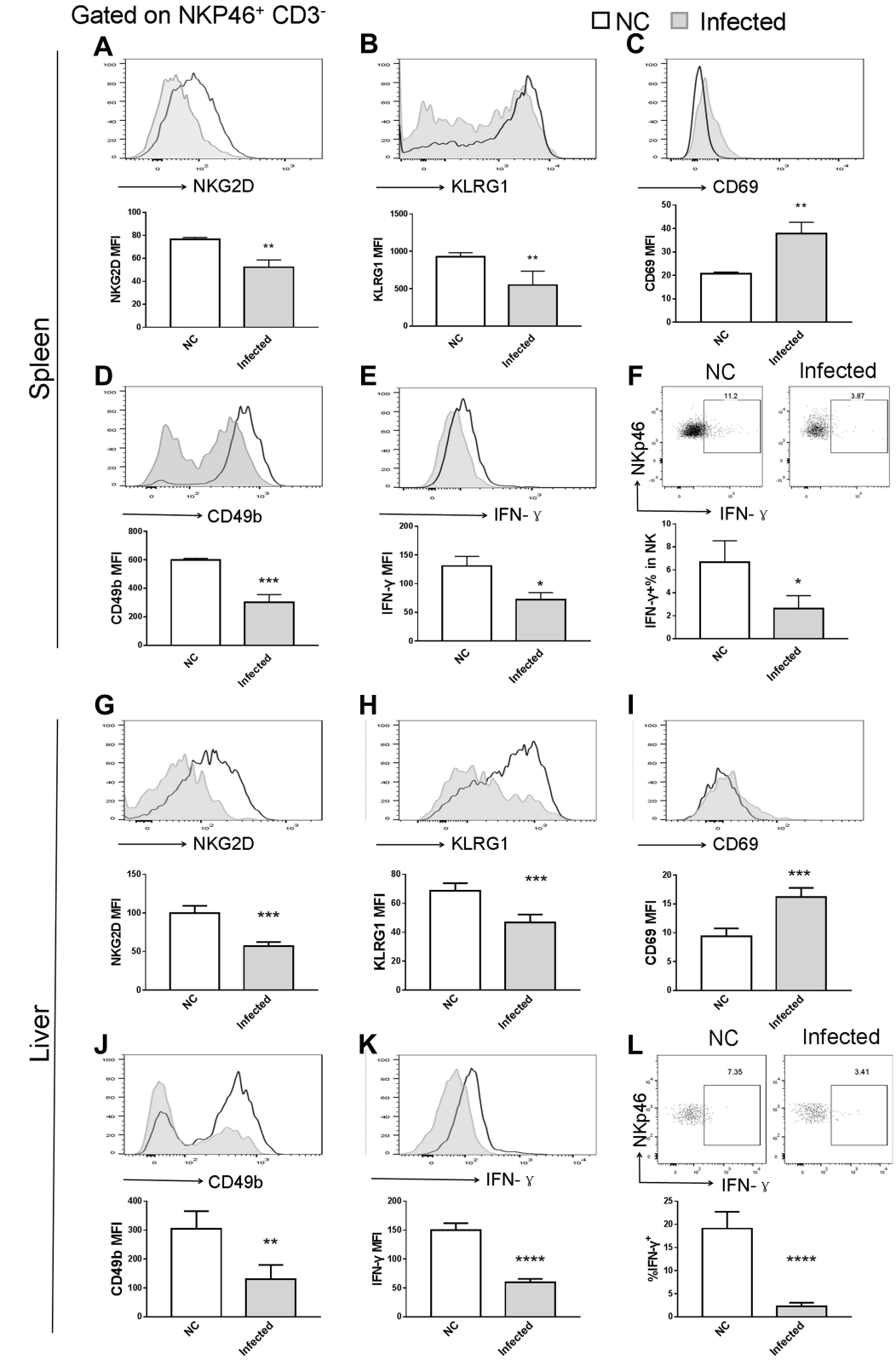

Figure 5 NK cell phenotype changes due to infection. Long term *S. japonicum* infection downregulated (**A** and **G**) NKG2D, (**B** and **H**) KLRG1 and (**D** and **J**) CD49b and (**E, F, K** and **L**) IFN-γ expression and elevated (**C** and **I**) CD69 level on NK cell surface. Open line, health control; filled grey line, infected in all representative histograms. Data are representative of 4–6 animals per subgroup and 3 independent experiments. Comparisons were between Infected and NC. *P<0.05, **P<0.01, ***P<0.001 and ****P<0.0001.

Abbreviations: NKG2D, natural killer group 2, member D receptor; KLRG1, killer cell lectin-like receptor G1.

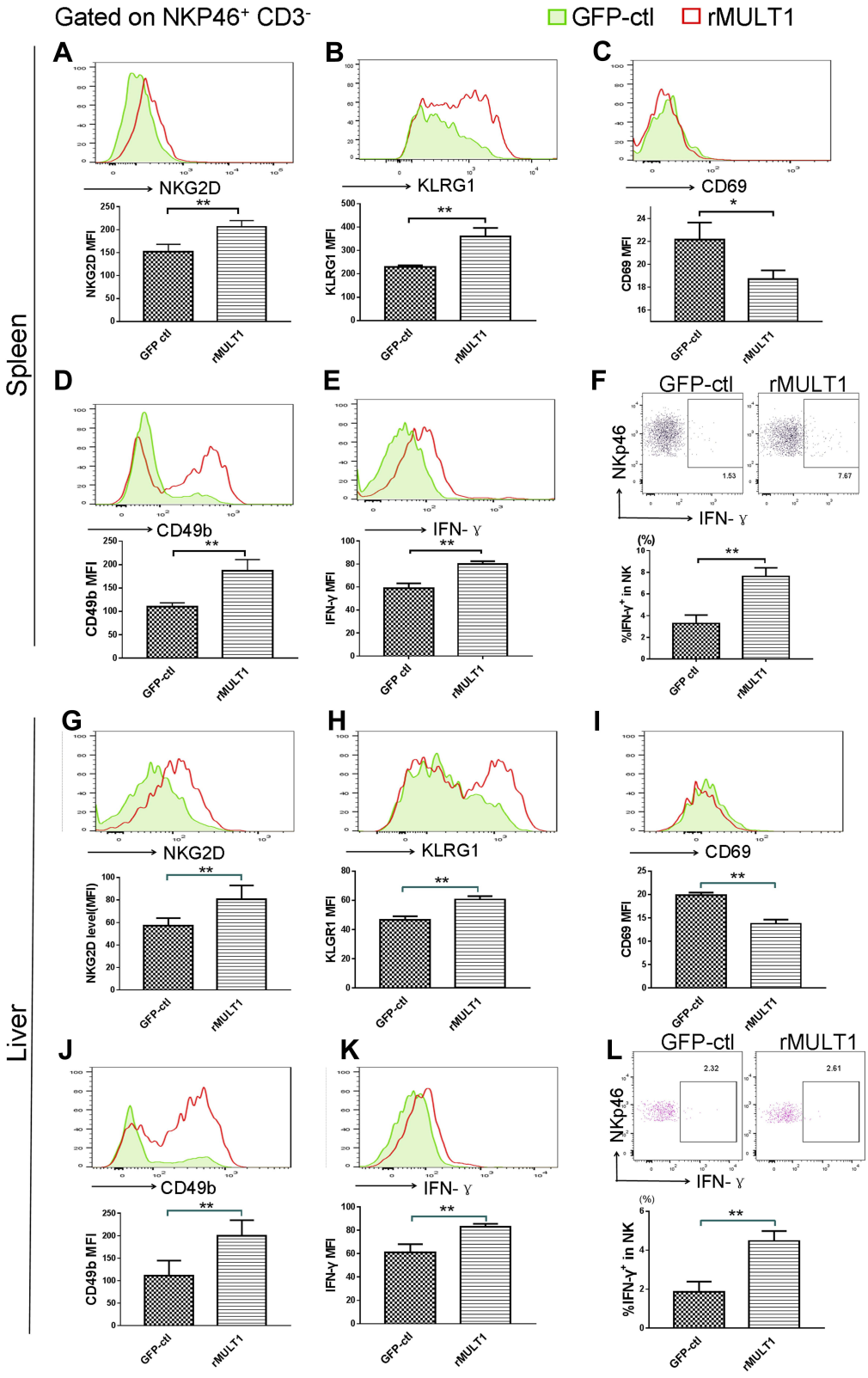

Figure 6 NK cell phenotype changes were restored by rMULT1 DNA treatment. NK cells form rMULT1 group showed increased (**A** and **G**) NKG2D, (**B** and **H**) KLRG1, (**D** and **J**) CD49b and decreased (**C** and **I**) CD69, as well as enhanced (**E, F, K** and **L**) IFN-γ secretion, compared to those from GFP-ctl group. Open red line, rMULT1 group; filled green line, GFP-ctl group in all representative histograms. Data are representative of 4–6 animals per subgroup and 3 independent experiments. Comparisons were between rMULT1 and GFP-ctl, *P<0.05 and **P<0.01.

Abbreviations: MULT1, murine UL16-binding protein-like transcript 1; NKG2D, natural killer group 2, member D receptor; KLRG1, killer cell lectin-like receptor G1.

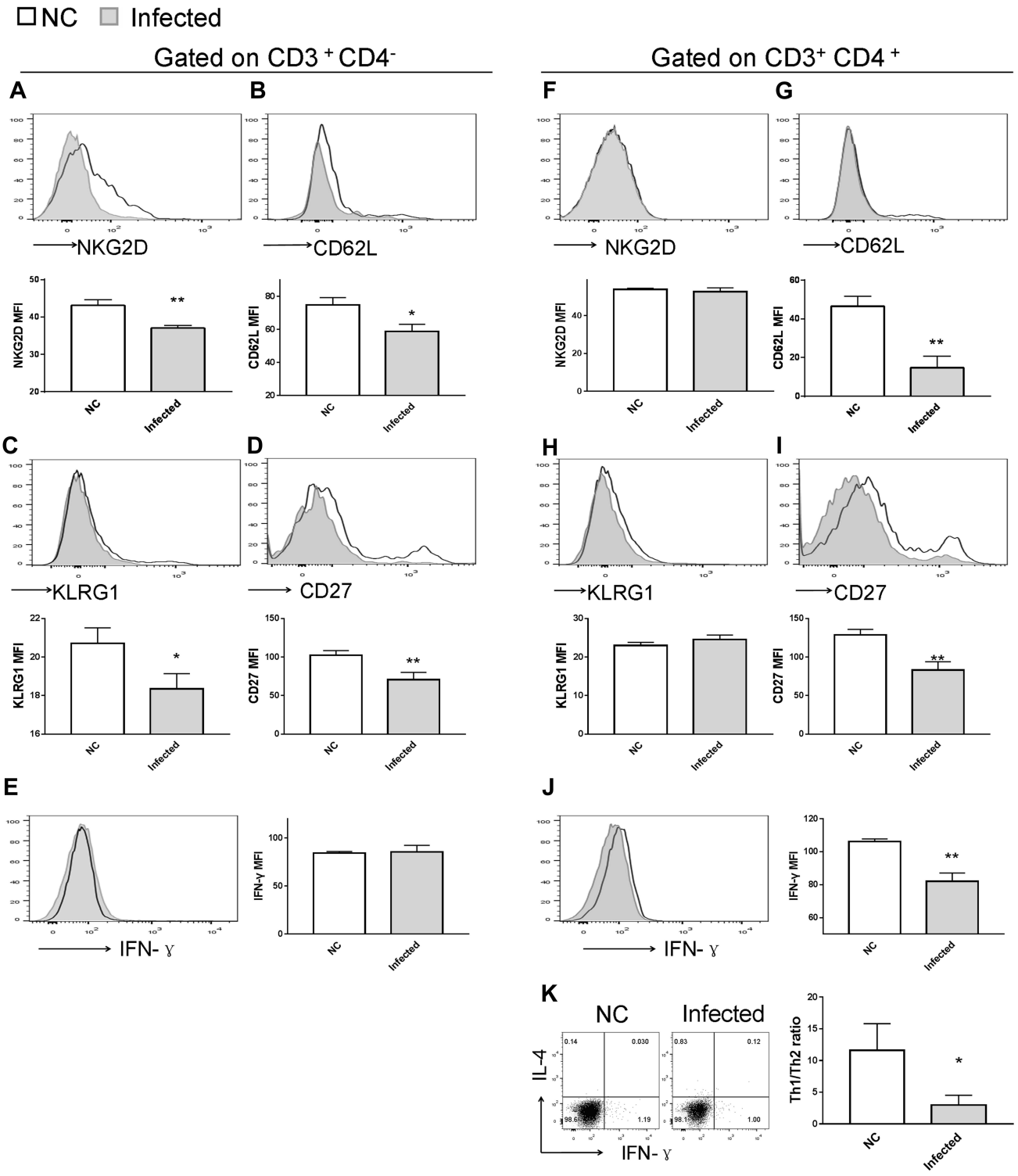

Figure 7 Impact of *S. japonicum* infection on splenic T-cell phenotype at the end of the 8th week post *S. japonicum* infection. Flow cytometry assay of (**A-E**) $CD8^+$ T cells and (**F-K**) $CD4^+$ T cells. Data demonstrated (**A** and **F**) suppressed NKG2D expression on $CD8^+$ T cells, but not on $CD4^+$ T cells from treated mice. Infected mice exhibited lower CD62L and lower CD27 expression both on (**G** and **I**) $CD4^+$ T and (**B** and **D**) $CD8^+$ T cells compared with control mice. (**C** and **H**) $CD8^+$ T cells, but not $CD4^+$ T cells, exhibited downregulated surface expression of KLRG1 upon *S. japonicum* infection, while (**E** and **J**) $CD4^+$ T cells, but not $CD8^+$ T cells, exhibited decreased IFN-γ secretion in the infected mice. (**K**) Combined staining of $CD4^+$ T cells with intracellular IFN-γ and IL-4 demonstrated a significant decrease of the Th1/Th2 ratio in the $CD4^+$ T cells of the infected mice. Open line, health control; filled grey line, infected in all representative histograms. Data are representative of 4–6 animals per subgroup and 3 independent experiments. Comparisons were between Infected and NC. *P<0.05 and **P<0.01.

Abbreviations: NKG2D, natural killer group 2, member D receptor; KLRG1, killer cell lectin-like receptor G1.

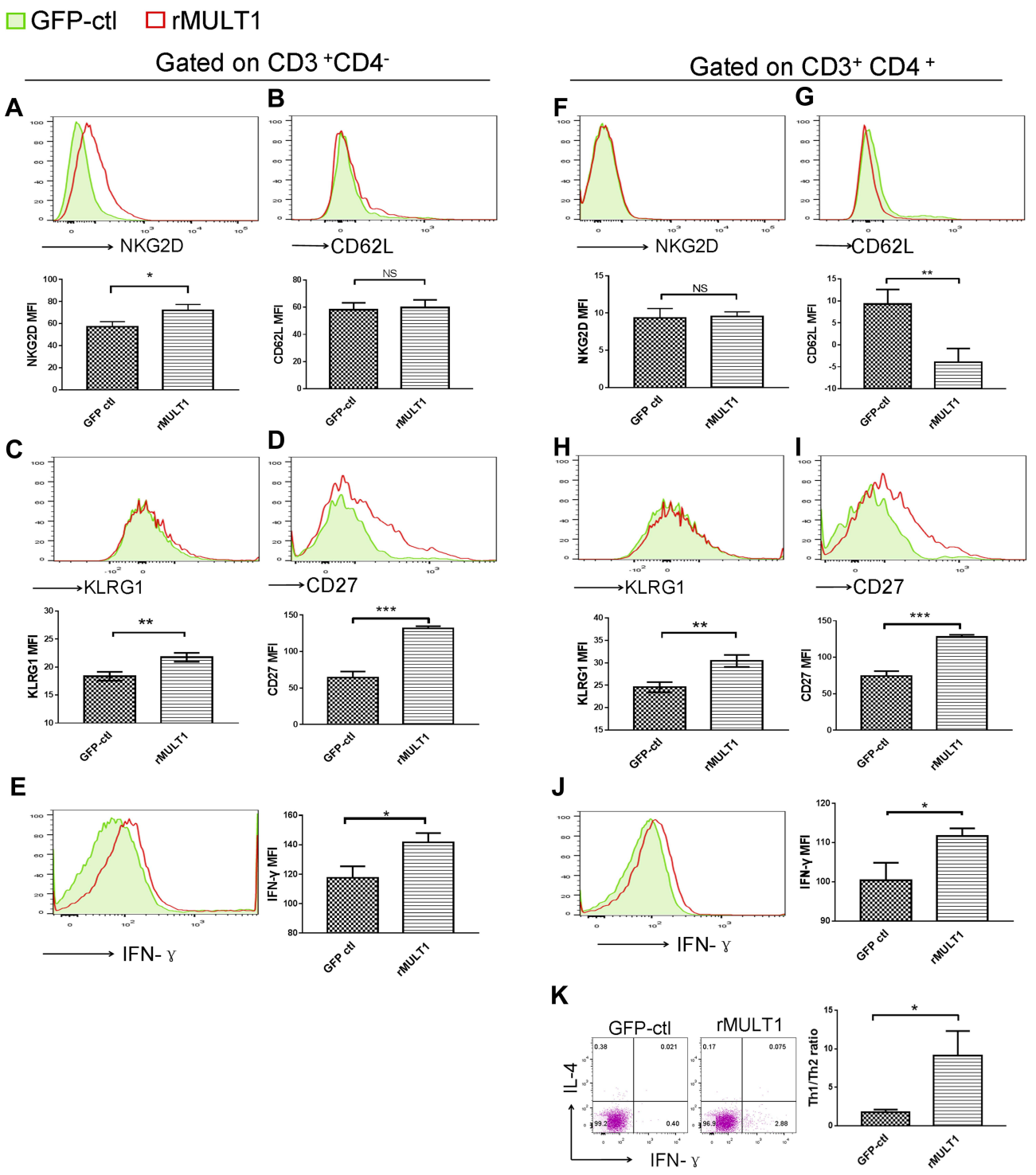

Figure 8 Impact of rMULT1 DNA treatment on splenic T-cell phenotype in mice with *S. japonicum* infection. Flow cytometry data demonstrated an elevated NKG2D expression on (**A**) $CD8^+$ T cells but not on (**F**) $CD4^+$ T cells from treated mice. (**G**) The treated group exhibited decreased CD62L expression on $CD4^+$ T cells compared with the GFP-ctl group, while (**B**) $CD8^+$ T cells exhibited similar surface level of CD62L. Both $CD8^+$ T and $CD4^+$ T cells exhibited increased surface expression of (**C** and **H**) KLRG1 and (**D** and **I**) CD27, as well as (**E** and **J**) enhanced IFN-γ secretion upon rMULT1 DNA treatment. (**K**) Combined staining of $CD4^+$ T cells with intracellular IFN-γ and IL-4 revealed a significantly higher Th1/Th2 ratio in $CD4^+$ T cells of the treated mice. Open red line, rMULT1 DNA; filled green line, vehicle DNA in all representative histograms. Data are representative of 4–6 animals per subgroup and 3 independent experiments. Comparisons were between rMULT1 and GFP-ctl, *P<0.05, **P<0.01 and ***P<0.001.

Abbreviations: MULT1, murine UL16-binding protein-like transcript 1; NKG2D, natural killer group 2 member D receptor; KLRG1, killer cell lectin-like receptor G1.

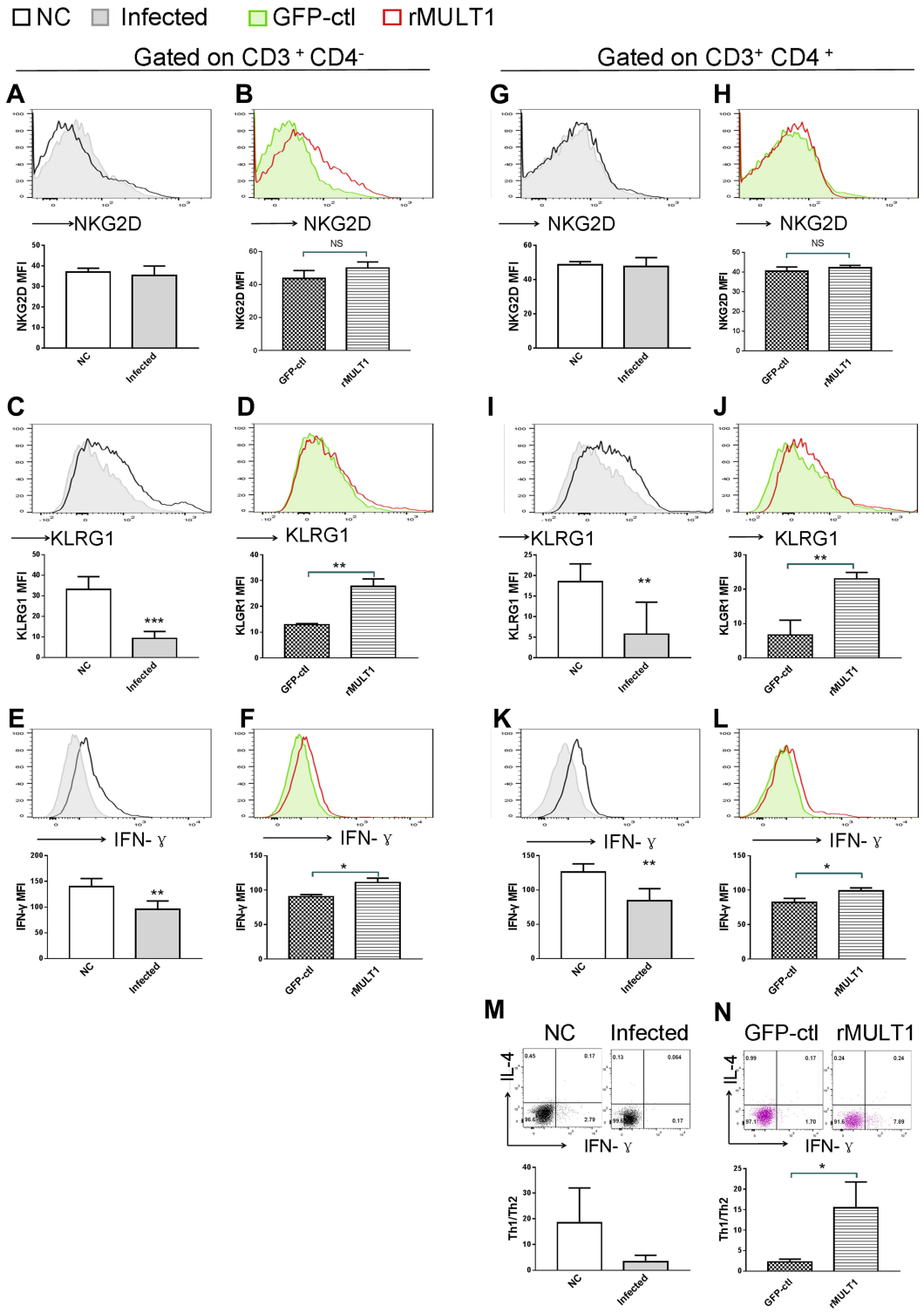

Figure 9 Impact of (**A, C, E, G, I, K, M**) infection and (**B, D, F, H, J, L, N**) rMULT1 DNA treatment on liver T-cell phenotype in mice with *S. japonicum* infection. Flow cytometry data revealed unchanged NKG2D levels on hepatic (**A and B**) $CD8^+$ T and (**G** and **H**) $CD4^+$ T cells in response to either (**A** and **G**) infection or (**B** and **H**) consequent treatment with rMULT1 DNA. Both $CD8^+$ T and $CD4^+$ T cells exhibited downregulated surface expression of (**C** and **I**) KLRG1 and (**E** and **K**) IFN-γ production upon *S. japonicum* infection, which were reversed by rMULT1 DNA treatment (**D, J, F** and **L**). (**M** and **N**) Combined staining of $CD4^+$ T cells with intracellular IFN-γ and IL-4 revealed (**M**) a significantly descent in Th1/Th2 ratio in liver $CD4^+$ T cells due to infection and (**N**) a restore of that in treated mice. Open dark line, health control; filled grey line, infected; open red line, rMULT1 DNA; filled green line, vehicle DNA in all representative histograms. Data are representative of 4–6 animals per subgroup and 3 independent experiments. Comparisons were between rMULT1 and GFP-ctl, *P<0.05, **P<0.01 and ***P<0.001.

Abbreviations: MULT1, murine UL16-binding protein-like transcript 1; NKG2D, natural killer group 2 member D receptor; KLRG1, killer cell lectin-like receptor G1.

These data indicated that treatment with rMULT1 DNA ameliorated T-cell homeostasis and modulated Th cell differentiation, facilitating the differentiation of effector $CD4^+$ T cells and delaying the Th1/Th2 shift during chronic infection with *S. japonicum*.

Discussion

In models of *S. japonicum* infection and CCl4-induced liver fibrosis, ex vivo evidence showed that NK cells can inhibit liver fibrosis in mice in an RAE/NKG2D-dependent manner.[28,46] IL-30, which can promote the expression of NKG2D on the surface of hepatic NKT cells, enhances the cytotoxic effect of NKT cells on activated HSCs and reduces liver fibrosis via the NKG2D/RAE-1 interaction.[47] Nevertheless, as a co-stimulatory receptor for the TCR/CD3 complex on the surface of activated T cells, NKG2D signal was also reported to promote injury-related inflammatory responses.[48] More solid evidence is in need to determine whether NKG2D-based immunity does good or does bad in liver fibrosis following lesion induced by *Schistosoma* infection. Among all known NKG2D ligands, MULT1 binds to mouse NKG2D with the highest affinity.[32] In our present study, we constructed a recombinant of MULT1 encoding plasmid, p-rMULT1. It was administered to BALB/c mice with *S. japonicum* infestation to investigate the role of MULT1 on mouse hepatic fibrosis induced by *Schistosoma* infection. Overexpression of rMULT1 in vivo using hydrodynamics-based transfection resulted in shrunk area of egg granuloma and fibrosis area around single egg. Collagen I and α-SMA in the liver of the infected mice were also reduced upon rMULT1 overexpression. Its overexpression also inhibited the body weight loss caused by *S. japonicum*. The therapy with rMULT1 DNA did not elicit cytokine storm or other obvious toxic and side effects demonstrated by unchanged survival, ALT level, colon length, as well as similar tissue morphology of multiple organs. Hence, MULT1 is a potential protective factor in schistosomiasis and over expression of MULT1 ameliorated schistosomiasis associated with hepatic fibrosis. To the best of our knowledge, the present study provides the first in vivo evidence of the potential value of NKG2D-based immunity elicited by its ligands in the treatment of schistosomiasis-associated hepatic fibrosis.

NK cell function has previously been shown to be inhibited during the fibrotic phase of schistosomiasis,[40] and the degree of liver fibrosis in mice infected with *S. mansoni* is exacerbated following treatment with anti-NK1.1 antibody to deplete $NK1.1^+$ ($CD3^+$ $NK1.1^+$ NKT and $CD3^-$ $NK1.1^+$ NK) cells,[49] suggesting that NKT and NK cells may negatively regulate egg-induced liver fibrosis. NK cell activation is concisely regulated by receptors falling into two categories: inhibitory receptors and stimulating receptors.[50,51] Among them, NKG2D is an extra strong activating receptor regarding that activating NKG2D signaling constitutes the molecular basis to override inhibitory signals from inhibitory NK receptors.[52] On the other hand, NKG2D, as well as CD49b, KLRG1 and CD69 are among the surface molecules for evaluating maturation stages, activation status of NK cells.[53–55] In our present work, NK cells were inhibited in expression of NKG2D, KLRG1, CD49b and IFN-γ and enhance in expression of CD69 by chronic *Schitosoma* infection and all the changes, both in spleen and in liver local, were inversely screwed by treatment with p-rMULT1, demonstrating restoration of NK cell function being involved in the mechanism by which p-rMULT1 attenuated *Schitosoma* induced fibrosis.

T-cell immunity is a well-known critical immune response against schistosomiasis and associated hepatic fibrosis.[16,56] Helper T cells are the majority of $CD4^+$ T cells and are divided into two major subtypes, Th1 and Th2. A shift from Th1 response to Th2 response occurs in the host along with the oviposition of schistosomes.[6,16] IL-4, a critical Th2 type cytokine, is a double-edge sword for schistosomiasis. On the one hand, it is indefensible for mice with *Schistosoma* infection to survive the acute phase.[9,57] On the other hand, it can enhance Th2 response and promote hepatic fibrosis.[7,10] Cutting down IL-4, but not absolutely deleting it, was proved to be effective in improving the health status of mice with schistosomiasis associated hepatic fibrosis[8] In our present work, we found that the expression of IFN-γ in splenic $CD4^+$ T, NKT, NK cells and in hepatic $CD8^+$ T cells was significantly enhanced in the p-rMULT1 treatment group, and the IFN-γ level in the liver was also elevated. In the meantime, IL-4 level either in the liver or in the serum did not change upon treatment. IFN-γ not only inhibits Th2 cell proliferation,[17] but also promotes Th1 cell differentiation[18] and inhibits HSC activation, and promotes apoptosis of HSCs by inhibiting the TGF-β signaling pathway, thus playing an important anti-fibrosis role.[19,20] Therefore, the results of the present study suggested that the reduction of liver fibrosis in the p-rMULT1 treatment group may be partially due to increased

activation of Th1 (IFN-γ^+ $CD4^+$ T) cells, resulting in downregulation of Th2 cell responses, or inhibition of liver fibrosis by IFN-γ secreted by lymphocytes, such as T cells, NKT and NK cells.

CD27 is one of the co-stimulatory receptors for T cells in both mice and humans, conducting stimulatory signals for T-cell activation in anti-infection and antitumor immune response.[58–61] While KLRG1 is considered to be a co-inhibitory receptor on lymphocytes,[62,63] it is also a surface marker of maturation for NK and T cells.[55,64,65] In a recent study, enhanced KLRG1 expression on $CD4^+$ T cells was observed upon treatment in tuberculosis patients who had lower $KLRG1^+$ $CD4^+$ T cells than healthy individuals, either with or without *Mycobacterium tuberculosis* infection.[64] $KLRG1^+$ $CD8^+$ T cells have been shown to exhibit high plasticity in developing into versatile memory cells, hence contributing to long-term protective immunity.[65] In the treated mice of our current study, surface KLRG1 expression was found to be increased in both types of T cells from spleen and liver, so as the CD27 expression of splenic T cells. In line with the largely adverse changes in the expression of these molecules due to *S. japonicum* infection, it appears that rMULT1 DNA treatment modulated T-cell homeostasis. These observations indicate that modulating T-cell responses may be another important mechanism mediating the effects of the rMULT1 DNA treatment against schistosomiasis-associated hepatic fibrosis.

Given the fact that NKG2D-signal and NK cell activation are efficient in eliciting Th1 immune response and increasing IFN-γ secretion,[27] while NKG2D is absent in CD4+ T cells and only transduces co-stimulating signal to CD8+ T cells,[38,39] NK cells might play as a trigger in the cellular mechanism of p-rMULT employing screwed NK cell, CD4+ T cells, CD8+ T cells and others to alleviate murine schistosomiasis-associated hepatic fibrosis, which is yet to be confirmed by further investigations using appropriate specific depletion or defection models.

Conclusion

In summary, by administering *S. japonicum* infected mice with a recombinant plasmid encoding MULT1, the strongest ligand for stimulating NKG2D, we demonstrate that overexpressed MULT1 is promising in treating experimental hepatic fibrosis induced by. *S. japonicum*, and involved mechanisms include increased proportion and function of NKG2D-expressing lymphocytes, ameliorated NK- and T-cell homeostasis, improved cellular immunity and modulated Th cell differentiation as well as regulated T (Th)1/Th2 balance. Our findings proposed a new potential therapy against schistosomiasis associated with liver fibrosis by targeting NKG2D signaling.

Abbreviations

α-SMA, α-smooth muscle actin; HA, hemagglutinin; HSCs, hepatic stellate cells; KLRG1, killer cell lectin-like receptor G1; MICA, MHC class I chain-related family molecules A; MULT1, murine ULBP-like transcript 1; NKG2D, natural killer group 2 member D receptor; rMULT1, recombinant MULT1; p-rMULT1, plasmid encoding recombinant MULT1; RAE, retinoic acid early transcript; ULBP, unique long 16-binding protein.

Acknowledgments

The present study was supported by the National Natural Science Foundation of China (grant nos. 81772221 and 81672047), Fundamental Research Funds for the Central Universities (HUST: grant nos. 2015QN147, 2017KFYXJJ056), the Natural Science Foundation of Hubei Province, China (grant no. 2016CFB419), and the Foundation of Health and Family Planning Commission of Hubei Province, China (grant no. WJ2017X006).

Disclosure

The authors report no conflicts of interest in this work.

References

1. Mondiale de laSanté O; World Health Organization. Schistosomiasis: number of people treated worldwide in 2014. *Wkly Epidemiol Rec*. 2016;91(5):53–60.
2. Colley DG, Bustinduy AL, Secor WE, King CH. Human schistosomiasis. *Lancet*. 2014;383(9936):2253–2264.
3. Colley DG, Secor WE. Immunology of human schistosomiasis. *Parasite Immunol*. 2014;36(8):347–357.

4. Burke ML, Jones MK, Gobert GN, Li YS, Ellis MK, McManus DP. Immunopathogenesis of human schistosomiasis. *Parasite Immunol*. 2009;31(4):163–176.
5. Wynn TA, Thompson RW, Cheever AW, Mentink-Kane MM. Immunopathogenesis of schistosomiasis. *Immunol Rev*. 2004;201:156–167.
6. Pearce EJ, MacDonald AS. The immunobiology of schistosomiasis. *Nat Rev Immunol*. 2002;2(7):499–511.
7. Fairfax K, Nascimento M, Huang SCC, Everts B, Pearce EJ. Th2 responses in schistosomiasis. *Semin Immunopathol*. 2012;34(6):863–871.
8. Cheever AW, Finkelman FD, Cox TM. Anti-interleukin-4 treatment diminishes secretion of Th2 cytokines and inhibits hepatic fibrosis in murine schistosomiasis japonica. *Parasite Immunol*. 1995;17(2):103–109.
9. Brunet LR, Finkelman FD, Cheever AW, Kopf MA, Pearce EJ. IL-4 protects against TNF-alpha-mediated cachexia and death during acute schistosomiasis. *J Immunol*. 1997;159(2):777–785.
10. Fallon PG, Richardson EJ, McKenzie GJ, McKenzie ANJ. Schistosome infection of transgenic mice defines distinct and contrasting pathogenic roles for IL-4 and IL-13: is a profibrotic agent. *J Immunol*. 2000;164(5):2585–2591.
11. Sugimoto R, Enjoji M, Nakamuta M, et al. Effect of IL-4 and IL-13 on collagen production in cultured LI90 human hepatic stellate cells. *Liver Int*. 2005;25(2):420–428.
12. Liu Y, Meyer C, Muller A, et al. IL-13 Induces Connective Tissue Growth Factor in Rat Hepatic Stellate Cells via TGF-beta-Independent Smad Signaling. *J Immunol*. 2011;187(5):2814–2823.
13. Figueiredo AL, Domingues AL, Melo WG, et al. Receptor antagonist of IL-13 exerts a potential negative regulation during early infection of human schistosomiasis. *Scand J Immunol*. 2016;84(5):284–290.
14. Chiaramonte MG, Donaldson DD, Cheever AW, Wynn TA. An IL-13 inhibitor blocks the development of hepatic fibrosis during a T-helper type 2-dominated inflammatory response. *J Clin Invest*. 1999;104(6):777–785.
15. Liu TJ, Dhanasekaran SM, Jin H, et al. FIZZ1 stimulation of myofibroblast differentiation. *Am J Pathol*. 2004;164(4):1315–1326.
16. Zheng B, Zhang J, Chen H, et al. T lymphocyte-mediated Liver immunopathology of schistosomiasis. *Front Immunol*. 2020;11:61.
17. Chung F. Anti-inflammatory cytokines in asthma and allergy: interleukin-10, interleukin-12, interferon-gamma. *Mediators Inflamm*. 2001;10(2):51–59.
18. Radhakrishnan S, Wiehagen KR, Pulko V, et al. Induction of a Th1 response from Th2-polarized T cells by activated dendritic cells: dependence on TCR: peptide-MHC interaction, ICAM-1, IL-12, and IFN-gamma (Retracted article. See vol. 184, pg. 6555, 2010). *J Immunol*. 2007;178(6):3583–3592.
19. Baroni GS, D'Ambrosio L, Curto P, et al. Interferon gamma decreases hepatic stellate cell activation and extracellular matrix deposition in rat liver fibrosis. *Hepatology*. 1996;23(5):1189–1199.
20. Ulloa L, Doody J, Massague J. Inhibition of transforming growth factor-beta/SMAD signalling by the interferon-gamma/STAT pathway. *Nature*. 1999;397(6721):710–713.
21. Jamieson AM, Diefenbach A, McMahon CW, Xiong N, Carlyle JR, Raulet DH. The role of the NKG2D immunoreceptor in immune cell activation and natural killing. *Immunity*. 2002;17(1):19–29.
22. Groh V, Bruhl A, El-Gabalawy H, Nelson JL, Spies T. Stimulation of T cell autoreactivity by anomalous expression of NKG2D and its MIC ligands in rheumatoid arthritis. *Proc Natl Acad Sci U S A*. 2003;100(16):9452–9457.
23. Zafirova B, Wensveen FM, Gulin M, Polic B. Regulation of immune cell function and differentiation by the NKG2D receptor. *Cell Mol Life Sci*. 2011;68(21):3519–3529.
24. Bauer S, Groh V, Wu J, et al. Activation of NK cells and T cells by NKG2D, a receptor for stress-inducible MICA. *Science*. 1999;285(5428):727–729.
25. Rincon-Orozco B, Kunzmann V, Wrobel P, Kabelitz D, Steinle A, Herrmann T. Activation of V gamma 9V delta 2 T cells by NKG2D. *J Immunol*. 2005;175(4):2144–2151.
26. Nielsen MM, Dyring-Andersen B, Schmidt JD, et al. NKG2D-dependent activation of dendritic epidermal T cells in contact hypersensitivity. *J Invest Dermatol*. 2015;135(5):1311–1319.
27. Lu S, Zhang J, Liu D, et al. Nonblocking monoclonal antibody targeting soluble MIC revamps endogenous innate and adaptive antitumor responses and eliminates primary and metastatic tumors. *Clin Cancer Res*. 2015;21(21):4819–4830.
28. Hou X, Yu F, Man S, et al. Negative regulation of *Schistosoma japonicum* egg-induced liver fibrosis by natural killer cells. *PLoS Negl Trop Dis*. 2012;6(1):e1456.
29. Gong Z, Luo QZ, Lin L, et al. Association of MICA gene polymorphisms with liver fibrosis in schistosomiasis patients in the Dongting Lake region. *Braz J Med Biol Res*. 2012;45(3):222–229.
30. Basher F, Dhar P, Wang X, et al. Antibody targeting tumor-derived soluble NKG2D ligand sMIC reprograms NK cell homeostatic survival and function and enhances melanoma response to PDL1 blockade therapy. *J Hematol Oncol*. 2020;13(1):74.
31. Ferrari de Andrade L, Kumar S, Luoma AM, et al. Inhibition of MICA and MICB shedding elicits NK-cell-mediated immunity against tumors resistant to cytotoxic T cells. *Cancer Immunol Res*. 2020;8(6):769–780.
32. Carayannopoulos LN, Naidenko OV, Fremont DH, Yokoyama WM. Cutting edge: murine UL16-binding protein-like transcript 1: a newly described transcript encoding a high-affinity ligand for murine NKG2D. *J Immunol*. 2002;169(8):4079–4083.
33. Liu F, Song Y, Liu D. Hydrodynamics-based transfection in animals by systemic administration of plasmid DNA. *Gene Ther*. 1999;6(7):1258–1266.
34. Zhang G, Budker V, Wolff JA. High levels of foreign gene expression in hepatocytes after tail vein injections of naked plasmid DNA. *Hum Gene Ther*. 1999;10(10):1735–1737.
35. Lisi PJ, Huang CW, Hoffman RA, Teipel JW. A fluorescence immunoassay for soluble antigens employing flow cytometric detection. *Clin Chim Acta*. 1982;120(2):171–179.
36. Chuah C, Jones MK, Burke ML, McManus DP, Gobert GN. Cellular and chemokine-mediated regulation in schistosome-induced hepatic pathology. *Trends Parasitol*. 2014;30(3):141–150.
37. Bai Y, Guan F, Zhu F, et al. IL-33/ST2 axis deficiency exacerbates hepatic pathology by regulating Treg and Th17 cells in murine schistosomiasis japonica. *J Inflamm Res*. 2021;14:5981–5998.
38. Long EO. Versatile signaling through NKG2D. *Nat Immunol*. 2002;3(12):1119–1120.
39. Raulet DH. Roles of the NKG2D immunoreceptor and its ligands. *Nat Rev Immunol*. 2003;3(10):781–790.

40. Hu Y, Wang X, Wei Y, et al. Functional inhibition of natural killer cells in a BALB/c mouse model of liver fibrosis induced by *Schistosoma japonicum* infection. *Front Cell Infect Microbiol*. 2020;10:598987.
41. Xiao J, Guan F, Sun L, et al. B cells induced by *Schistosoma japonicum* infection display diverse regulatory phenotypes and modulate CD4(+) T cell response. *Parasit Vectors*. 2020;13(1):147.
42. Chen D, Xie H, Cha H, et al. Characteristics of *Schistosoma japonicum* infection induced IFN-gamma and IL-4 co-expressing plasticity Th cells. *Immunology*. 2016;149(1):25–34.
43. Stojanovic A, Correia MP, Cerwenka A. The NKG2D/NKG2DL axis in the crosstalk between lymphoid and myeloid cells in health and disease. *Front Immunol*. 2018;9:827.
44. Wilson MS, Mentink-Kane MM, Pesce JT, Ramalingam TR, Thompson R, Wynn TA. Immunopathology of schistosomiasis. *Immunol Cell Biol*. 2007;85(2):148–154.
45. Xu F, Cheng R, Miao S, et al. Prior *Toxoplasma gondii* infection ameliorates liver fibrosis induced by *Schistosoma japonicum* through inhibiting Th2 response and improving balance of intestinal flora in mice. *Int J Mol Sci*. 2020;21:8.
46. Radaeva S, Sun R, Jaruga B, Nguyen VT, Tian ZG, Gao B. Natural killer cells ameliorate liver fibrosis by killing activated stellate cells in NKG2D-dependent and tumor necrosis factor-related apoptosis-inducing ligand-dependent manners. *Gastroenterology*. 2006;130(2):435–452.
47. Mitra A, Satelli A, Yan J, et al. IL-30 (IL27p28) attenuates liver fibrosis through inducing NKG2D-Rae1 interaction between NKT and activated hepatic stellate cells in mice. *Hepatology*. 2014;60(6):2027–2039.
48. Strid J, Sobolev O, Zafirova B, Polic B, Hayday A. The intraepithelial T cell response to NKG2D-ligands links lymphoid stress surveillance to atopy. *Science*. 2011;334(6060):1293–1297.
49. Asseman C, Pancre V, Quatennens B, Auriault C. *Schistosoma mansoni*-infected mice show augmented hepatic fibrosis and selective inhibition of liver cytokine production after treatment with anti-NK1.1 antibodies. *Immunol Lett*. 1996;54(1):11–20.
50. Kumar S. Natural killer cell cytotoxicity and its regulation by inhibitory receptors. *Immunology*. 2018;154(3):383–393.
51. Lanier LL. Up on the tightrope: natural killer cell activation and inhibition. *Nat Immunol*. 2008;9(5):495–502.
52. Watzl C. The NKG2D receptor and its ligands-recognition beyond the "missing self"? *Microbes Infect*. 2003;5(1):31–37.
53. Stokic-Trtica V, Diefenbach A, Klose CSN. NK cell development in times of innate lymphoid cell diversity. *Front Immunol*. 2020;11:813.
54. Vosshenrich CA, Di Santo JP. Developmental programming of natural killer and innate lymphoid cells. *Curr Opin Immunol*. 2013;25(2):130–138.
55. Huntington ND, Tabarias H, Fairfax K, et al. NK cell maturation and peripheral homeostasis is associated with KLRG1 up-regulation. *J Immunol*. 2007;178(8):4764–4770.
56. Cheng YL, Song WJ, Liu WQ, Lei JH, Kong Z, Li YL. The effects of interleukin (IL)-12 and IL-4 deficiency on worm development and granuloma formation in *Schistosoma japonicum*-infected mice. *Parasitol Res*. 2012;110(1):287–293.
57. Schwartz C, Oeser K, Prazeres da Costa C, Layland LE, Voehringer D. T cell-derived IL-4/IL-13 protects mice against fatal *Schistosoma mansoni* infection independently of basophils. *J Immunol*. 2014;193(7):3590–3599.
58. van Lier RA, Borst J, Vroom TM, et al. Tissue distribution and biochemical and functional properties of Tp55 (CD27), a novel T cell differentiation antigen. *J Immunol*. 1987;139(5):1589–1596.
59. Gravestein LA, Nieland JD, Kruisbeek AM, Borst J. Novel mAbs reveal potent co-stimulatory activity of murine CD27. *Int Immunol*. 1995;7(4):551–557.
60. Kobata T, Jacquot S, Kozlowski S, Agematsu K, Schlossman SF, Morimoto C. CD27-CD70 interactions regulate B-cell activation by T cells. *Proc Natl Acad Sci U S A*. 1995;92(24):11249–11253.
61. Grant EJ, Nussing S, Sant S, Clemens EB, Kedzierska K. The role of CD27 in anti-viral T-cell immunity. *Curr Opin Virol*. 2017;22:77–88.
62. Robbins SH, Nguyen KB, Takahashi N, Mikayama T, Biron CA, Brossay L. Cutting edge: inhibitory functions of the killer cell lectin-like receptor G1 molecule during the activation of mouse NK cells. *J Immunol*. 2002;168(6):2585–2589.
63. Greenberg SA, Kong SW, Thompson E, Gulla SV. Co-inhibitory T cell receptor KLRG1: human cancer expression and efficacy of neutralization in murine cancer models. *Oncotarget*. 2019;10(14):1399–1406.
64. Tonby K, Mortensen R, Ruhwald M, Dyrhol-Riise AM, Jenum S. KLRG1-expressing CD4 T cells are reduced in tuberculosis patients compared to healthy *Mycobacterium tuberculosis*-infected subjects, but increase with treatment. *J Infect Dis*. 2019;220(1):174–176.
65. Herndler-Brandstetter D, Ishigame H, Shinnakasu R, et al. KLRG1(+) effector CD8(+) T cells lose KLRG1, differentiate into all memory T cell lineages, and convey enhanced protective immunity. *Immunity*. 2018;48(4):716–729 e718.